applied sciences

MDPI

Article

The Protective Effects of Unripe Apple (*Malus pumila*) Extract on Ultraviolet B-Induced Skin Photoaging Mouse Model

Hye Rim Park [1,†], Jae Kwang Kim [2,3,†], Jae Kyoung Lee [4,5], Beom Rak Choi [6], Sae Kwang Ku [1] and Kyung Hwan Jegal [7,*]

[1] Department of Anatomy and Histology, College of Korean Medicine, Daegu Haany University, Gyeongsan 38610, Republic of Korea
[2] Korean Medicine-Application Center, Korea Institute of Oriental Medicine, Daegu 41062, Republic of Korea
[3] Department of Physiology, College of Korean Medicine, Daegu Haany University, Gyeongsan 38610, Republic of Korea
[4] CNS Pharm Korea Co., Ltd., Seoul 04043, Republic of Korea
[5] Department of Food Regulatory Science, College of Science and Technology, Korea University, Sejong Campus, Sejong 30019, Republic of Korea
[6] Nutracore Co., Ltd., Suwon 16514, Republic of Korea
[7] Department of Korean Medical Classics, College of Korean Medicine, Daegu Haany University, Gyeongsan 38610, Republic of Korea
* Correspondence: jegalkh@dhu.ac.kr; Tel.: +82-53-819-1862
† These authors contributed equally to this work.

Abstract: An unripe apple (immature fruit of *Malus pumila* Mill) contains more polyphenols than mature fruit. To explore the anti-photoaging effects of unripe apple extract (UAE), we investigated the effects of UAE on wrinkle improvement, skin moisturizing, skin inflammation, and antioxidant activities using the ultraviolet B (UVB)-irradiated SKH1-hr hairless mouse model. The mice were irradiated with UVB (0.18 J/cm^2) three times per week and orally administrated UAE (100, 200, or 400 mg/kg) once a day for 15 weeks. The administration of UAE significantly prevented UVB-induced wrinkle formation and skin water loss, potentially by increasing the effects of UAE on type I collagen (COL1) and hyaluronic acid through the transcriptional regulation of COL1α (*COL1A1* and *COL1A2*), hyaluronan synthesis (*HAS1*, *HAS2*, and *HAS3*) and the matrix metalloproteinase (*MMP1*, *MMP9*, and *MMP13*) gene. Moreover, UAE significantly reduced UVB-induced skin edema, infiltrated neutrophils, and pro-inflammatory cytokine interleukin-1β (IL-1β), while increasing the anti-inflammatory cytokine IL-10. UAE also exerted anti-oxidative stress properties by increasing the glutathione content and inhibiting lipid peroxidation and superoxide anion production. The histopathological analysis demonstrated that UAE-induced anti-inflammation, anti-oxidative stress, and anti-apoptotic properties on the UVB-irradiated skin tissues. Therefore, UAE may be an effective natural resource to mitigate UVB-induced skin photoaging.

Keywords: skin photoaging; ultraviolet B; unripe apple

Citation: Park, H.R.; Kim, J.K.; Lee, J.K.; Choi, B.R.; Ku, S.K.; Jegal, K.H. The Protective Effects of Unripe Apple (*Malus pumila*) Extract on Ultraviolet B-Induced Skin Photoaging Mouse Model. *Appl. Sci.* **2023**, *13*, 4788. https://doi.org/10.3390/app13084788

Academic Editor: Anna Lante

Received: 9 March 2023
Revised: 7 April 2023
Accepted: 9 April 2023
Published: 11 April 2023

1. Introduction

Skin aging is typically distinguished by dryness, wrinkle formation, atrophy, sagging, rough texture, loss of elasticity, hyperpigmentation, and a thickened epidermis [1]. These changes, mainly observed in the dermal layer, are natural aging processes caused by sustained and irreversible degeneration of skin tissue, yet are also consequences of repeated exposure to sunlight, ultraviolet rays (UVR), drinking, smoking, and chemical toxins. Especially in skin areas exposed to sunlight, such as the face, neck, and the back of our hands, significant alterations are induced, such as wrinkle formation, spider veins, epidermal atrophy, melanogenesis, irregular pigmentation, and sunburn [2,3]. Among the spectrum of sunlight, UVA (320–400 nm) and UVB (280–320 nm) are the main causes of photoaging [3]. Depending on its wavelength, UVA penetrates through the dermis, and

causes deterioration and sagging, whereas UVB is absorbed in the epidermis and is the main cause of wrinkle formation [3,4]. At the cellular level, UVR induces DNA and RNA damage, protein mutation, inflammation, and an imbalance in the extracellular matrix (ECM) remodeling through intracellular reactive oxygen species (ROS) production [3].

Over the previous decades, as the public interest in skin beauty and health has increased and the related industries have grown exponentially, functional products have been developed to prevent skin aging and maintain healthy skin conditions, including antioxidants, whiteners, moisturizers, wrinkle improvers, and UV protectors [5]. However, safety issues are continuously raised regarding harmful chemicals and toxins, which are potential risk factors for chemical syntheses or metal-based skin products. Consequently, there is an extensive demand to develop functional materials for the skin using natural resources, including effective and safe medicinal plants and herbs. Vitamin C (L-ascorbic acid, L-AA), an abundant compound in fruits and vegetables, is well-known for its beneficial effects on skin health and diseases. L-AA has been reported to exert skin wrinkle improvement and UV protection through skin epidermal barrier formation by collagen, elastin, and ceramide syntheses, skin-moisturizing effects, antioxidant effects, and skin-whitening effects through the inhibition of melanogenesis [6]. An apple, a mature fruit of the deciduous tree of the Rosaceae family (*Malus pumila* Mill.), contains various beneficial ingredients for health, such as dietary fibers, vitamins, and polyphenols. Accumulating evidence shows that these abundant bioactive components in apples exert beneficial effects on lipid metabolism, cardiovascular diseases, and allergic diseases, as well as skin health [7–10]. Polyphenols are known to exert a potent ROS scavenging effect and anti-photoaging effect through inhibition of MMPs, elastase, and hyaluronidase [11]. Moreover, a recent study investigated the polyphenol applied with nanotechnology to exert antioxidant and UV protection effects that were superior than those of its parental polyphenol without cytotoxicity and genotoxicity [12]. A recent study revealed that both unripe and ripe apples contain various bioactive phenolic compounds such as chlorogenic acid, chlorogenic acid methyl ester, isoquercitrin, phloridzin, phloretin, quercitrin, and reynoutrin [13]. The content of total phenolic compounds in unripe apples is four times higher than that in the ripe apples [13]. Unripe apples also contain higher amounts of chlorogenic acid, 5-*O*-*p*-courmaroylquinic acid, and phloridzin compared to ripe apples [13]. Oral intake or topical application of polyphenol-rich plant extracts can contribute to delaying the aging process of the skin [11]. Therefore, an unripe apple is expected to be a promising candidate as a functional food ingredient for the skin. In this study, we investigated the effects of unripe apple extracts (UAEs) on wrinkle improvement, skin moisturizing, anti-inflammation, and antioxidant activities using an UVB-irradiated skin photoaging hairless mouse model, as compared with L-AA, to evaluate the possibility of a skin protection agent or functional food ingredient for skin.

2. Materials and Methods

2.1. Preparation of UAE

UAE was supplied by Nutracore (Suwon, Republic of Korea). UAE was prepared by crushing 100 kg of the harvested unripe apples at 55–65 days after full bloom, pressing, and filtering the juice, and then concentrating it using an evaporator (98 °C, 30 min, −120 mbar). The collected 5.25 kg of concentrate was mixed with dextrin (Sigma-Aldrich, St. Louis, MO, USA) and dried using a spray dryer (inlet 190 °C, outlet 100 °C, flow rate = 2 L/min) to obtain a light-yellow-colored powdered final product of 12 kg of UAE (Table S1). High-performance liquid chromatographic (HPLC) analysis showed that one peak of UAE matched with phloridzin (Sigma-Aldrich) at a retention time of approximately 26.453 min, and UAE contained 0.06 mg/g phloridzin (Figure S1).

2.2. Animal Experiment

The animal experiments were conducted in accordance with the National Institute of Health Guide for the Care and Use of Laboratory Animals and approved by the Institutional

Animal Care and Use Committee of the Daegu Haany University (Approval No. DHU2021-030). SKH1-hr hairless mice (Female, 6 weeks old, n = 10 per group) were supplied by Orient Bio (Seongnam, Republic of Korea) and acclimatized in a condition-controlled room (22–25 °C, 40–60% relative humidity, and 12/12 h light/dark cycle) for 7 days. To induce skin photoaging by UVB irradiation, the mice were exposed to UVB (0.18 J/cm^2) three times per week for 15 weeks using a UV Crosslinker system (CL-1000M, Analytik Jena, Upland, CA, USA) emitting wavelengths of 254 nm, 312 nm, and 365 nm with peak emission at 312 nm. Unexposed intact control mice were placed in an off-emitting Crosslinker system for the identical duration as that of UVB-exposed mice, to induce equivalent environmental stresses. After 1 h of UVB exposure, the mice were orally administrated UAE (100, 200 and 400 mg/kg) dissolved in distilled water once a day for 105 days. L-ascorbic acid (L-AA, Sigma-Aldrich), widely known for its skin protection effect, was used as a positive control at an oral dose of 100 mg/kg. One day after final oral administration, the mice were sacrificed. The collected tissue sample was stored at −150 °C in an ultra-deep freezer (MDF-1156, Sanyo, Tokyo, Japan) until analysis.

2.3. Generation of Replicas and Assessment of Skin Wrinkle Formation

The replica of the dorsal skin was obtained using the Repliflo Cartridge Kit (CuDerm Corp., Dallas, TX, USA), and a photograph of the dorsal skin in the gluteal region was captured using a digital camera (FinePix S700, Fujifilm, Tokyo, Japan) prior to the sacrifice. The impression replicas were positioned on the horizontal sample stand, and wrinkle shadows were produced by stationary illumination at a 40° angle using an optical light source. A monochrome image was captured by a CCD camera, and the length and depth of wrinkles were measured in the skin replicas using a Skin-Visiometer system (SV600, Courage & Khazaka Electronics GmbH, Cologne, Germany).

2.4. Evaluation of Skin Water Contents and Skin Edema

Skin samples for evaluation of skin edema were collected by a punch with a constant area (6 mm diameter) from the dorsal back skin of mice. The result is presented as the mean weight of skin samples (g). The skin water contents were measured with the dorsal back skin tissue sample (6 mm diameter) using an Ohaus MB23 Moisture Analyzer (Prin Brook, NJ, USA). The content of skin water is presented as the percentage of total weight of skin tissue (%).

2.5. Measurement of Type I Collagen (COL1) Contents in Skin Tissue

One day after final oral administration, dorsal back skin tissue was collected, and the tissue was homogenized using a taco^{TM} Prep Bead Beater (GeneReach Biotechnology Corp., Taichung, Taiwan) and ultrasonic cell disruptor (KS-750, Madell Technology Corp., Ontario, CA, USA). After being dissolved in radioimmunoprecipitation assay (RIPA) buffer (Sigma-Aldrich), the supernatant was separated by centrifugation (15,000× g, 30 min, 4 °C). Quantitative measurement was conducted using a Procollagen type I C-peptide (PIP) EIA kit (Takara Bio, Tokyo, Japan), following the instructions of the manufacturer.

2.6. Measurement of Hyaluronic Acid Contents in Skin Tissue

To measure the hyaluronic acid content, the collected dorsal skin tissue was degreased with acetone, boiled in 50 mM Tris/HCl (pH 7.8) buffer for 20 min, and then added to 1% actinase E (Sigma-Aldrich) proteolytic digestion solution for a week at 40 °C. Next, the sample was mixed with trichloroacetic acid (10% w/v at final concentration, Sigma-Aldrich) for deproteinization, and the supernatant was separated by centrifugation (3000× g, 20 min, 4 °C). The separated supernatant was neutralized with 10 N NaOH. Hyaluronic acid contents were quantified using a mouse hyaluronic acid enzyme-linked immunosorbent assay (ELISA) kit (Mybiosource, San Diego, CA, USA), following the instructions of the manufacturer.

2.7. Assessment of Skin Myeloperoxidase (MPO) Activity

MPO kinetic-colorimetric assay was conducted for evaluating UVB-induced neutrophil inflammatory response [14]. The tissue sample was homogenized using a bead beater and ultrasonic cell disruptor in a buffer solution (50 mM, pH 6.0) containing 0.5% hexadecyl trimethyl-ammonium bromide (Gibco, Carlsbad, CA, USA). The homogenate was centrifuged (1000× *g* for 2 min at 4 °C), and the supernatant was recollected. The supernatant was mixed with K_2HPO_4 buffer (50 mM, pH 6.0), containing *o*-dianisidine dihydrochloride (0.167 mg/mL, Sigma-Aldrich) and 0.05% hydrogen peroxide. The absorbance was determined using a UV/Vis spectrophotometer (OPTIZEN POP, Mecasys, Daejeon, Republic of Korea) at 450 nm. The Lowry method was employed to measure the protein levels in the skin homogenates. The MPO activity of samples was compared to a standard curve of neutrophils. The results are presented as MPO activity (number of total neutrophils/mg of protein).

2.8. Measurement of IL-1β and IL-10 in Skin Tissue

IL-1β and IL-10 contents in the dorsal back skin tissue were measured using mouse IL-1β (ab100705; Abcam, Cambridge, UK) and IL-10 (ab108870; Abcam) ELISA kits, following the manufacturer's protocol. Briefly, the homogenized tissue sample was centrifuged (1236R, Labogene, Daejeon, Republic of Korea) at 14,000× *g* for 20 min with 0.1 M phosphate-buffered saline containing 1% Triton X-100. The supernatants were incubated in the plate for 2 h, washed, and further incubated with biotinylated IL-1β or IL-10 antibody for 2 h. The absorbance was measured using a microplate reader (Sunrise, Tecan, Männedorf, Switzerland) at 450 nm.

2.9. Evaluation of Antioxidant Activities (Measurement of Glutathione (GSH) Level, Lipid Peroxidation and Superoxide Anion Production)

To determine GSH level in skin tissue, the sample was homogenized in 100 mM NaH_2PO_4 (pH 8.0) containing 5 mM EDTA. The homogenates were treated with 30% trichloroacetic acid and centrifuged twice (at 1940× *g* for 6 min and at 485× *g* for 10 min). The supernatant was mixed with *o*-phthalaldehyde (1 mg/mL in methanol). The fluorescence intensity of the supernatant was measured using a fluorescence spectrophotometer (RF-5301PC, Shimadzu Corp., Tokyo, Japan) (k_{exc} = 350 nm; k_{em} = 420 nm). Results are expressed as μM of GSH/mg of protein as compared with a standard curve prepared with GSH (0.0–75.0 μM). Thiobarbituric acid reactive substances (TBARS) assay for detecting malondialdehyde (MDA), a commonly used biomarker for lipid peroxidation, was conducted to determine lipid peroxidation. Briefly, the skin tissue homogenate was mixed with trichloroacetic acid (10%, Sigma-Aldrich) to precipitate proteins and centrifuged (1000× *g*, 3 min). The extracted clear protein-free supernatant was incubated with thiobarbituric acid (0.67%) at 100 °C for 15 min. MDA was determined by computing the difference between absorbances at 535 and 572 nm by a microplate reader (Tecan). Results were expressed as nM/mg of protein. To assess superoxide anion production in skin tissue (10 mg/mL in 1.15% KCl), the nitroblue tetrazolium (NBT) assay was employed. Briefly, the homogenate of skin tissue was incubated with NBT (1 mg/mL) at 37 °C for 1 h. The supernatant was removed, and the reduced formazan was solubilized by adding 2 M KOH and dimethyl sulfoxide. The NBT reduction by superoxide anion was observed at 600 nm using a microplate reader (Tecan). Data were normalized with the protein content.

2.10. Real-Time Polymerase Chain Reaction (PCR)

Dorsal back skin tissues were homogenized using a taco™ Prep Bead Beater (GeneReach Biotechnology Corp.). Total RNAs were isolated using TRIzol reagent (Invitrogen, Carlsbad, CA, USA). cDNA synthesis, real-time PCR, and relative quantification were performed as previously described [15,16]. Sequences of oligonucleotide primers are listed in Table S2. Data are represented as mean ± SD of groups of ten mice, relative to intact control/β-actin.

2.11. Histopathology and Immunohistochemistry

The collected sample from the dorsal back skin around the gluteal region was prepared in 10% neutral buffered formalin for 24 h and then embedded in a paraffin block. The paraffin block section (3–4 μm) was stained with hematoxylin and eosin for general histopathologic analysis, and with Masson's trichrome (MT) for collagen fibers. The histological profiles of the sample were observed using a light microscope (Eclipse 80i, Nikon, Tokyo, Japan), equipped with histological camera systems (ProgRes^{TM} C5, Jenoptik Optical Systems GmbH, Jena, Germany) and a computer-assisted automated image analyzer (iSolution FL ver 9.1, IMT isolution Inc., Vancouver, BC, Canada). The average count of formed microfolds on the epithelium surface (folds/mm of epithelium), epithelial thicknesses (μm/epithelium), and numbers of inflammatory cells that infiltrated the dermis (cells/mm^2 of dermis) were calculated. Immunohistochemical staining on the dorsal back skin tissue using anti-cleaved caspase-3, anti-poly(ADP-ribose) polymerase (PARP), anti-nitrotyrosine(NT), anti-4-hydroxynonenal (4-HNE), and anti-matrix metalloproteinase (MMP) 9 antibodies was conducted. Briefly, the sample sections were incubated with methanol and 0.3% H_2O_2 for 30 min to block endogenous peroxidase activity. After then, they were incubated in a humidity chamber with normal horse serum for 1 h to block non-specific binding of immunoglobulin after heat-based (95~100 °C) epitope retrievals in 10 mM citrate buffers (pH 6.0). Samples were incubated with primary antibodies overnight at 4 °C in a humidity chamber, and then incubated with biotinylated universal secondary antibody and avidinbiotin-peroxidase complex reagents for 1 h. Samples were reacted with a peroxidase substrate kit (Vector Labs, Burlingame, CA, USA) for 3 min at room temperature. Epithelial cells with over 40% of immunoreactivity were considered as positive, and the mean number of cleaved caspase-3 and PARP and the number of NT and 4-HNE immunolabeled epithelial cells (%, cells/100 epithelial cells) were counted. The occupied percentages by MMP9 immunoreactive fibers were calculated in the dermis as %/mm^2. The histopathologist who performed the analysis was blind to group distribution.

2.12. Statistical Analysis

All data are presented as mean ± standard deviation (SD) of 10 hairless mice. For multiple comparison tests among experimental groups, statistical analysis was conducted using SPSS for Windows (Release 14.0 K, SPSS Inc., Armonk, NY, USA). The Levene test was used to examine variance homogeneity. To determine the significances of differences among experimental groups, one-way analysis of variance test was conducted, and followed by Tukey's HSD test for post hoc analysis to determine significant differences between pairs of groups. For nonparametric comparison test, the Kruskal–Wallis H test and Mann–Whitney *U* test were performed. Statistical significance was accepted for p-values < 0.05.

3. Results

3.1. Effect of UAE on Body Weight Changes

The average weight of the intact control (non-irradiated UVB mice) group was 25.03 ± 1.54 g one day before oral administration, and it decreased to 21.67 ± 1.19 g by the fasting on the start day of administration (Day 0). The average body weight of the intact control group gradually increased, reaching an average of 29.98 ± 2.31 g on the final day of administration (Day 104) (Figure 1). No significant differences were detected in body weights in the UVB-irradiated hairless mice compared with the non UVB-irradiated intact control group. Administration of UAE or L-AA produced no significant differences in body weight changes compared with the intact control or UVB group.

3.2. Effects of UAE on UVB-Induced Skin Wrinkle Formation and Skin Moisturization

To examine the effects of UAE on wrinkle formation in UVB-irradiated skin, the length and depth of skin wrinkles were measured using the replica of the dorsal back skin. Notably, exposure to UVB radiation resulted in significant skin wrinkles, which were mitigated by oral administration of either UAE or L-AA (Figure 2A). Moreover, the mean skin length

(mm) and depth (μm) after exposure to UVB (0.71 ± 0.08 mm and 102.18 ± 16.70 μm, respectively) were markedly elevated in contrast to the intact control (0.28 ± 0.07 mm, and 29.64 ± 12.03 μm, respectively). However, both UAE and L-AA significantly suppressed the formation of skin wrinkles in terms of length and depth (Figure 2B,C). Maintaining proper skin moisture is essential to protect skin from UVB-irradiated skin damage. UVB irradiation evidently decreased the skin water contents in the skin sample (13.22 ± 2.24%) compared to the intact control (35.95% ± 6.83%), which was significantly restored by both UAE and L-AA (Figure 2D). Hyaluronic acid and COL1 are key molecules that prevent skin wrinkle formation and maintain skin moisture. UAE and L-AA showed a significant increase in the reduced hyaluronic acid and COL1 contents by UVB exposure (Figure 2E,F). Moreover, the mRNA expression of COL1 and hyaluronic acid syntheses related genes (*COL1A* and *HAS*) were significantly increased by both UAE and L-AA (Figure 2G,H). To elucidate the effects of UAE on collagen degradation, the mRNA expression of the MMPs was quantified using real-time PCR analysis. The UVB-induced mRNA expression of *MMP1*, *MMP9*, and *MMP13* were significantly reduced by UAE and L-AA (Figure 2I). No significant differences were detected between the UAE- and L-AA treated mice receiving an equal oral dosage.

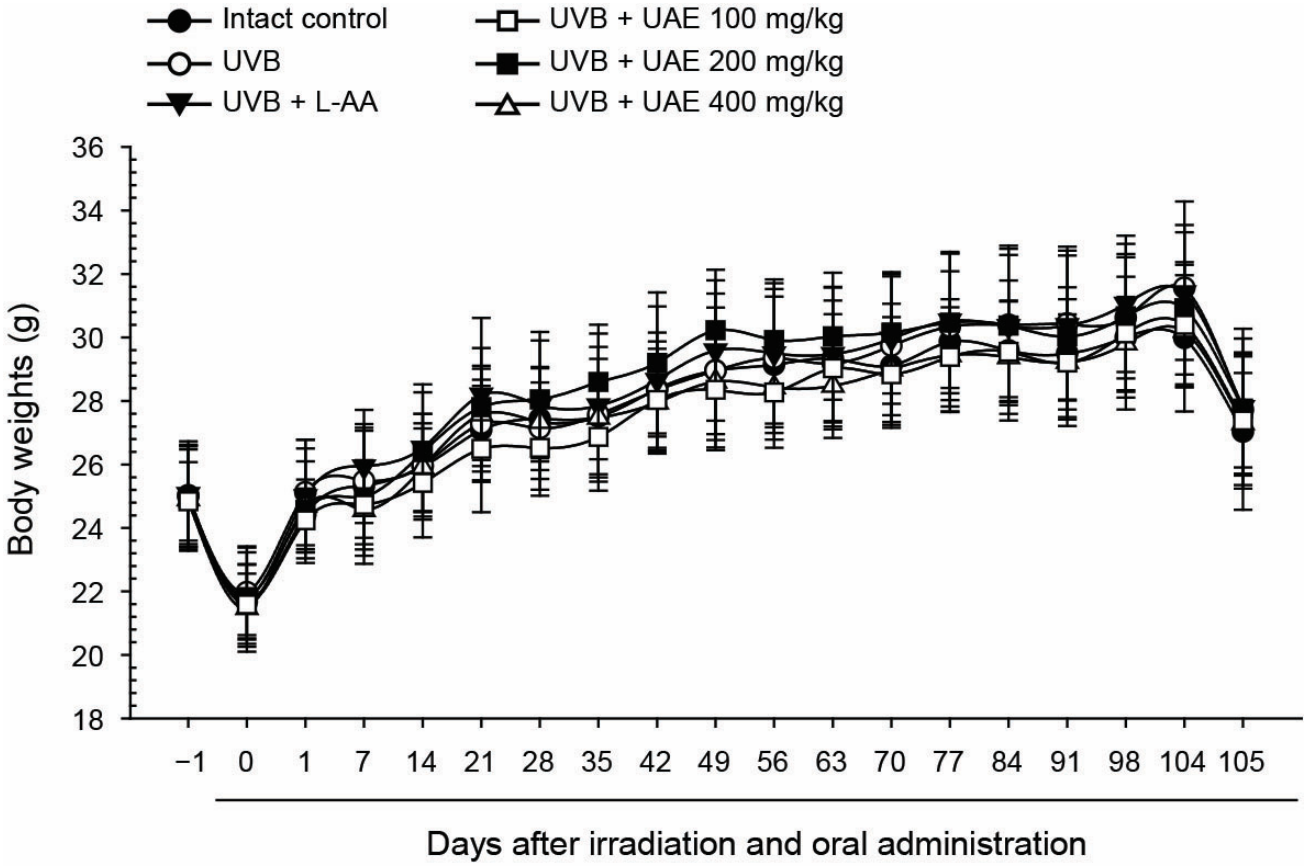

Figure 1. Bodyweight changes on the days after UVB irradiation and oral administration. The mice were irradiated to UVB (three times per week) or not for 15 weeks. UAE (100, 200, and 400 mg/kg) or L-AA (100 mg/kg) was orally administrated once a day for 105 days after 1 h of UVB irradiation. All mice were overnight fasted prior to both first administration and sacrifice. The body weights were measured every week. Data are represented as mean ± SD (n = 10, significance compared with intact control mice).

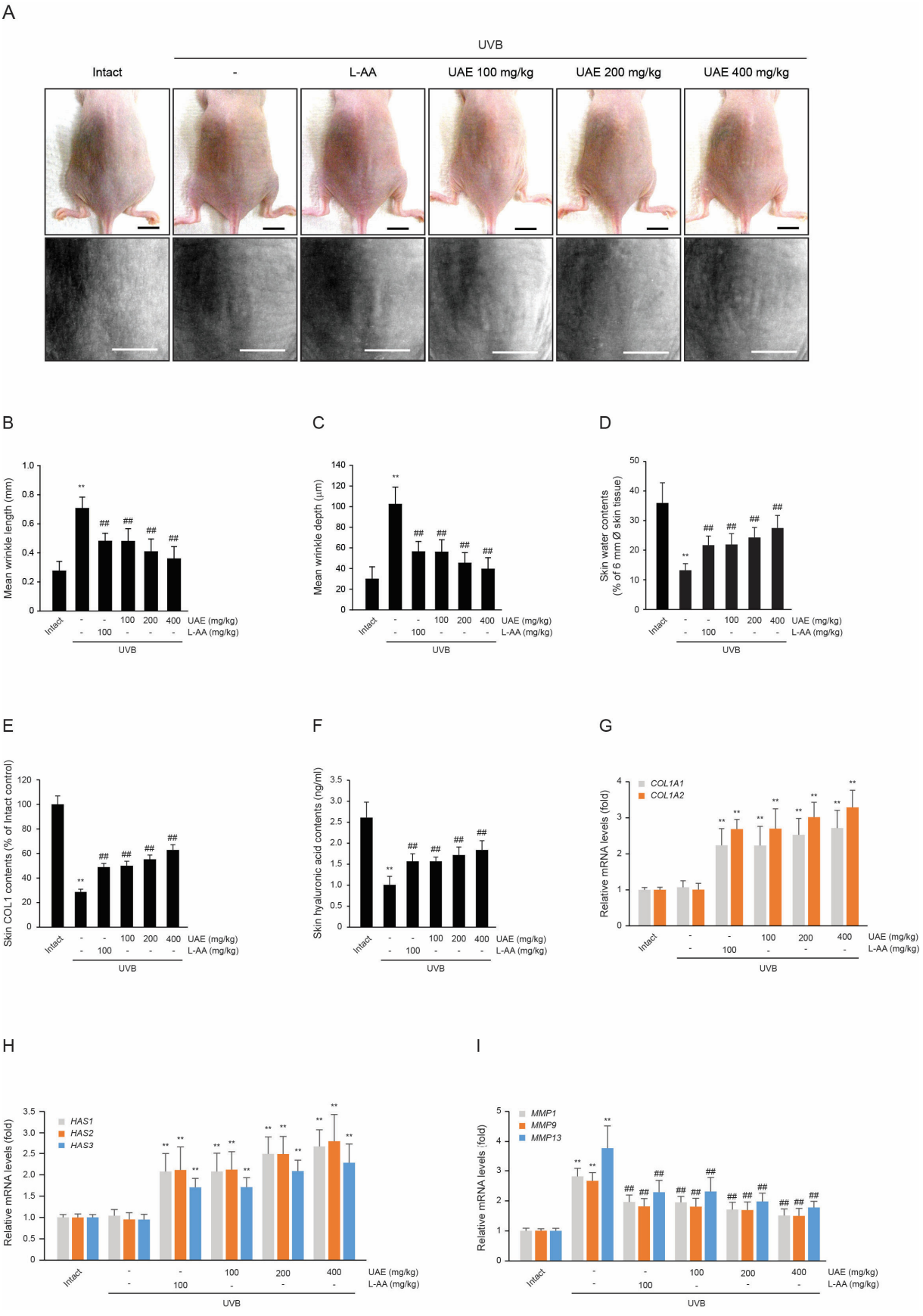

Figure 2. Effects of UAE on UVB-induced wrinkle formation in dorsal back skin. (**A**) Photograph of dorsal back skin (upper), Monochrome image of skin replicas (lower). Scale bars indicate10 mm. Wrinkle

shadows were generated using an optic light source by a fixed intensity at a 40° angle. (**B**,**C**) Wrinkle length and depth were measured in skin replicas. (**D**) Water contents in dorsal back skin tissues. Data are presented as a percentage of the total weight of the dorsal back skin tissue (6 mm diameter). (**E**) COL1 and (**F**) hyaluronic acid contents in dorsal back skin tissues. COL1 and hyaluronic acid contents were determined by ELISA assay. Data are presented as a percentage of intact control. (**G**) COL1 synthetic (*COL1A1* and *COL1A2*), (**H**) hyaluronic acid synthesis (*HAS1*, *HAS2*, and *HAS3*), and (**I**) MMP (*MMP1*, *MMP9*, and *MMP13*) gene expression in dorsal back skin tissues. mRNA expressions levels were quantified using the real-time PCR analysis. Data are expressed relative to intact/β-actin. Dorsal back skin was sampled at 24 h after the last day of administration. Results are presented as mean ± SD (n = 10, significant difference vs. intact control; ** $p < 0.01$, vs. UVB-irradiated control mice; ## $p < 0.01$).

3.3. Effects of UAE on UVB-Induced Skin Inflammation

Sustained exposure to UVB irradiation results in skin inflammation, which causes erythema, swelling, edema, and itching. To evaluate the effect of UAE on skin edema, 6 mm diameter skin samples were weighed. The increased weights of skin samples due to UVB irradiation were significantly reduced by UAE and L-AA (Figure 3A). In addition, UVB significantly increased MPO activity, a biomarker for skin neutrophil content, which was also significantly attenuated by UAE and L-AA (Figure 3B). Compared with the intact control, UVB significantly induced increased levels of IL-1β in the skin tissues, a cytokine-stimulating neutrophil, whereas it significantly decreased IL-10, an anti-inflammatory cytokine. However, such changes in cytokines in the skin tissue due to UVB irradiation were evidently reversed by UAE and L-AA (Figure 3C). There were no significant differences between the UAE and L-AA treated mice groups receiving an equal oral dosage.

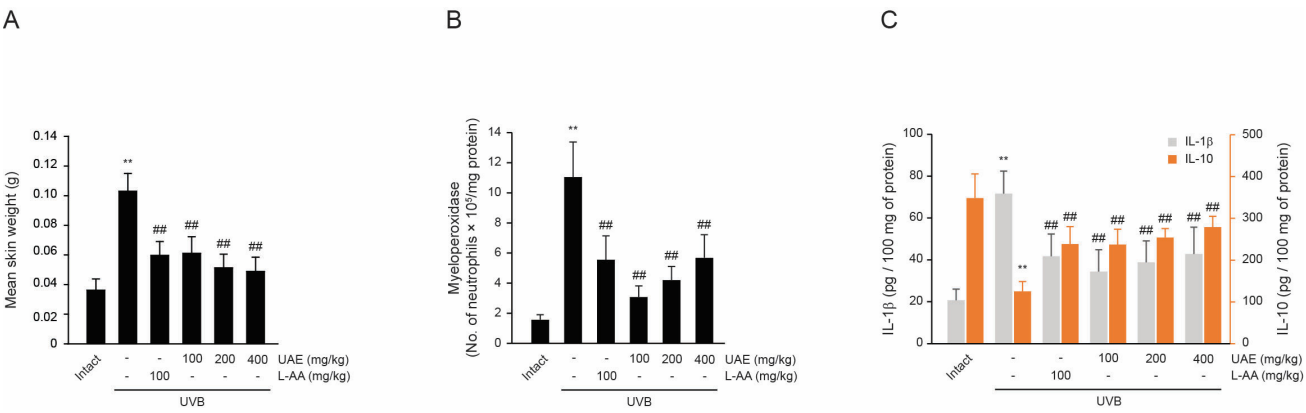

Figure 3. Effects of UAE on UVB-induced skin inflammation. (**A**) Skin edema was evaluated with the weight of a constant area (6 mm diameter) of dorsal back of mice. Data are presented as mean weight of skin samples (g). (**B**) Myeloperoxidase (MPO) activities for skin neutrophil content, and (**C**) IL-1β and IL-10 levels were determined in dorsal back skin tissue. Results are presented as mean ± SD (n = 10, significant difference vs. intact control; ** $p < 0.01$, vs. UVB-irradiated control mice; ## $p < 0.01$).

3.4. Effects of UAE on UVB-Induced Oxidative Stress

To explore the effects of UAE on antioxidant activities in skin tissue, the GSH, MDA, and superoxide anion levels were determined. GSH content was significantly decreased by UVB compared to the intact control, while it was increased by UAE and L-AA (Figure 4A). Moreover, administration of UAE or L-AA also significantly attenuated UVB-induced lipid peroxidation (MDA levels) and superoxide anion production (Figure 4B,C). To determine the oxidative stress-related gene expressions (*GSH reductase* and *NOX2*), real-time PCR analysis was conducted. UVB irradiation decreased *GSH reductase* mRNA expression and serves to maintain GSH by reducing GSSG; however, this was significantly alleviated by

UAE and L-AA (Figure 4D). In addition, the expression of UVB-induced *NOX2* mRNA, an enzyme associated with NADPH oxidase-derived ROS generation, was significantly reduced by UAE or L-AA treatments (Figure 4E). At the equal oral dosage level, there were no significant differences between the UAE- and L-AA treated mice groups in terms of antioxidant properties in the present study.

3.5. Effects of UAE on UVB-Induced Histopathological Changes in Skin Tissue

Histopathological analysis revealed that the thickened epithelial tissue resulted from the hyperplasia/hypertrophy of epidermal keratinocytes, microfold formation on the surface of the epithelial lining, and infiltration of inflammatory cells into the dermis in UVB-irradiated dorsal back skin tissue, as observed with hematoxylin and eosin stains. Masson's trichrome staining also showed abnormal collagen deposition due to UVB irradiation. However, these histopathological changes were significantly mitigated in the dorsal back skin tissues of UAE or L-AA treated mice (Figure 5A and Table 1). Furthermore, UAE or L-AA ameliorated UVB-induced immunolabeled cells for oxidative stress (NT and 4-HNE) and apoptosis (cleaved caspase3 and cleaved PARP) in the epidermis, and immunoreactive cells for MMP9 in the dermis (Figure 5B and Table 2). No significant differences were detected between the UAE- and L-AA treated mice receiving an equal oral dosage.

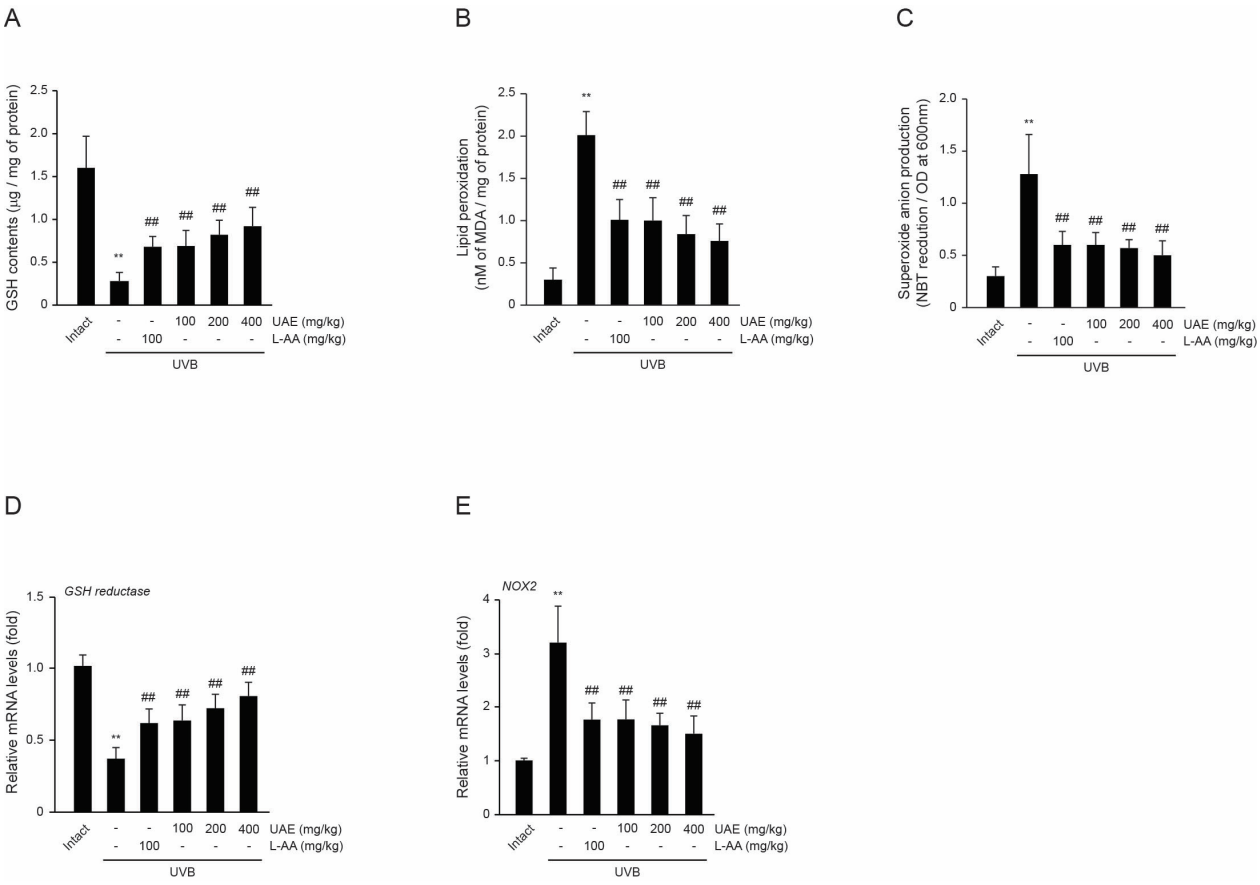

Figure 4. Effects of UAE on UVB-induced oxidative stress. (**A**) GSH contents, (**B**) malondialdehyde (MDA), and (**C**) superoxide anion production was measured in the skin tissues. Data were normalized by total proteins in the skin tissue. (**D**) *GSH reductase* (**E**) *NOX2* mRNA expression levels in dorsal back skin tissue were quantified by real-time PCR. Data are expressed relative to intact/b-actin. Results are presented as mean ± SD (n = 10, significant difference vs. intact control; ** $p < 0.01$, vs. UVB-irradiated control mice; ## $p < 0.01$).

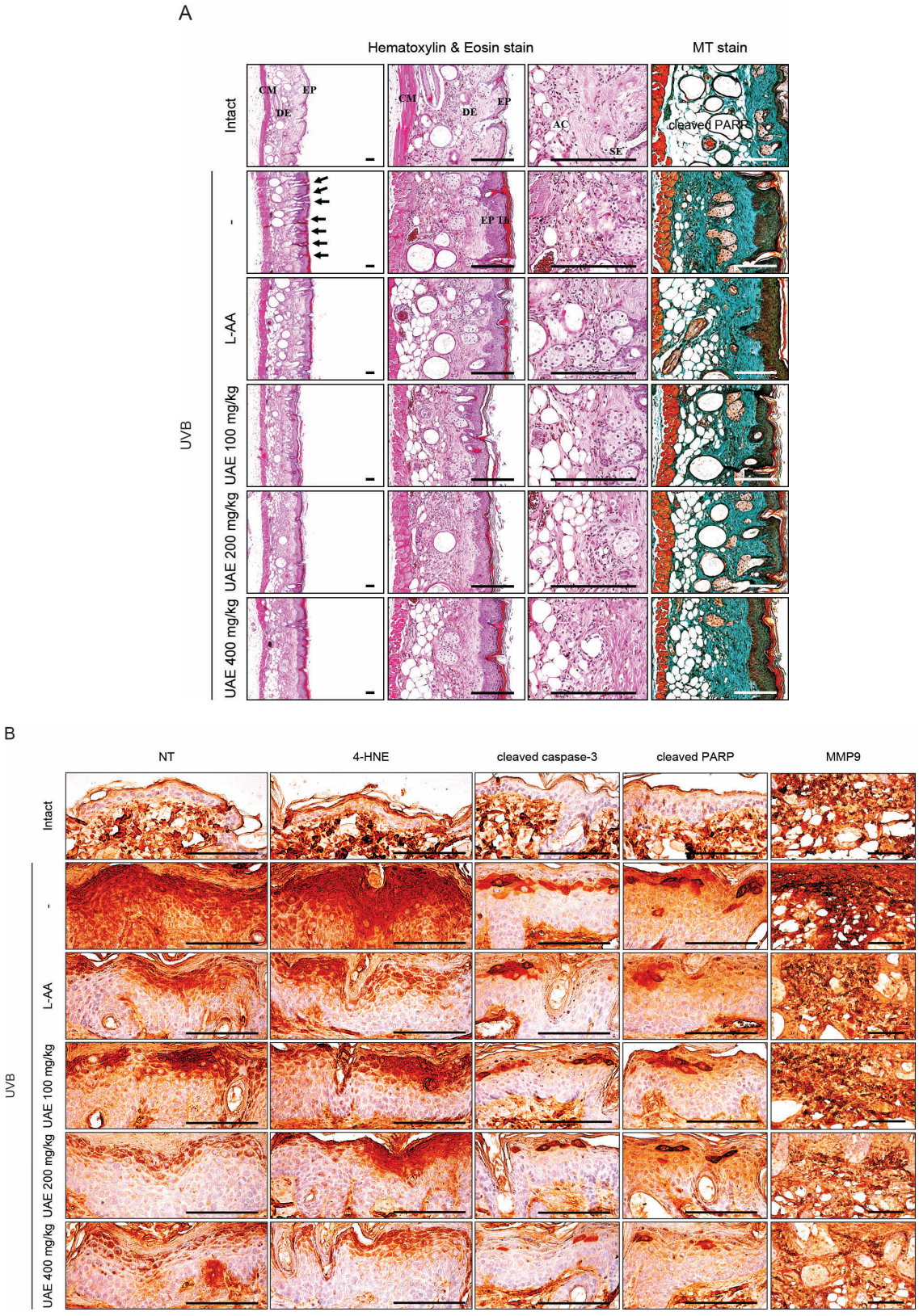

Figure 5. (**A**) Representative images of stained skin tissue with hematoxylin and eosin or Masson's trichrome (MT). Arrows indicate microfolds in skin epithelial surface. Scale bars indicate 200 μm. (**B**) Immuno-stained skin tissue using nitrotyrosine (NT), 4-hydroxynonenal (4-HNE), cleaved caspase-3, cleaved PARP, and MMP9 antibodies. Scale bars indicate 100 μm. EP, epithelium; DE, dermis; CM, cutaneous muscle; SE, sebaceous gland; AC, adipocyte; Th, thickness.

Table 1. Histopathological changes in UVB-irradiated dorsal back skin tissue.

Groups \ Iteme(Unit)	Number of Microfolds (Folds/mm of Epidermis)	Mean Epithelial Thickness (μm/Epidermis)	Mean Inflammatory Cells (cells/mm^2 of Dermis)	Collagen Fiber Occupied Regions (%/mm^2 of Dermis)
Intact	4.50 ± 0.97	30.59 ± 2.98	31.00 ± 10.38	35.41 ± 5.06
UVB	18.90 ± 2.73 **	114.18 ± 13.78 **	260.80 ± 65.34 **	78.86 ± 4.21 **
L-AA 100 mg/kg	12.50 ± 1.72 ##	78.56 ± 10.00 ##	159.80 ± 17.32 ##	59.68 ± 10.75 ##
UAE 100 mg/kg	12.70 ± 1.34 ##	77.69 ± 10.98 ##	162.40 ± 16.54 ##	60.15 ± 10.43 ##
UAE 200 mg/kg	10.80 ± 1.93 ##	65.49 ± 12.69 ##	129.80 ± 27.12 ##	52.96 ± 10.10 ##
UAE 400 mg/kg	8.50 ± 2.01 ##	62.89 ± 11.44 ##	88.60 ± 19.32 ##	47.32 ± 12.42 ##

Samples were stained with hematoxylin and eosin for general histopathology, and with Masson's trichrome (MT) for collagen fibers. Data are expressed as mean ± SD of 10 hairless mice. ** $p < 0.01$, compared with the non-UVB exposed intact control; ## $p < 0.01$, compared with the UVB group.

Table 2. Immuno-histological changes in UVB-irradiated dorsal back skin tissue.

Items \ Groups	Intact	UVB	L-AA 100 mg/kg	UAE 100 mg/kg	UAE 200 mg/kg	UAE 400 mg/kg
Epidermis (cells/100 epithelial cells)						
Nitrotyrosine	14.80 ± 5.90	69.10 ± 11.34 **	46.40 ± 11.73 ##	47.00 ± 10.51 ##	32.40 ± 11.27 ##	28.40 ± 10.28 ##
4-HNE	22.20 ± 6.56	75.60 ± 10.78 **	52.40 ± 7.88 ##	52.20 ± 11.94 ##	41.80 ± 10.35 ##	38.20 ± 10. ##
Cleaved caspase-3	4.00 ± 2.11	35.60 ± 10.36 **	24.00 ± 5.16 ##	24.80 ± 3.55 ##	17.40 ± 4.62 ##	10.80 ± 3.79 ##
Cleaved PARP	3.60 ± 2.07	39.70 ± 10.02 **	26.20 ± 2.74 ##	24.90 ± 3.48 ##	13.80 ± 4.47 ##	8.40 ± 2.46 ##
Dermis (%/mm^2)						
MMP9	18.63 ± 4.88	54.47 ± 10.14 **	37.54 ± 4.32 ##	37.65 ± 4.01 ##	30.15 ± 5.37 ##	26.72 ± 3.59 ##

Data are expressed as mean ± SD of 10 hairless mice. ** $p < 0.01$, compared with the non-UVB exposed intact control; ## $p < 0.01$, compared with the UVB group; 4-HNE, 4-Hydroxynonenal; PARP, poly(ADP-ribose) polymerase; MMP, Matrix metalloprotea.

4. Discussion

As the demand for anti-skin aging treatments increases, functional products for skin, such as whiteners, anti-wrinkle treatments, moisturizers, and UV protectors, are being developed. The skin functional product industry, including cosmetics and dietary supplements, is already one of the highest-valued market areas, and is continuing to grow. In particular, the market for natural-compound-based products is growing more rapidly than the overall market [5]. Unripe apple is known to be rich in polyphenols and an excellent source of natural antioxidants [17]. However, 20–30% of unripe apples are discarded every year, which causes economic and environmental problems in Korea [18]. Therefore, various methods to create value using the remaining unripe apples are required. In this study, we tried to explore the effects of UAE in preventing UVB-irradiated skin photoaging.

Chronic exposure to UVB leads to ROS generation, inflammation, and increased cytokines and chemokines, which result in a deterioration in the barrier function of skin and the deepening of wrinkles through the degradation of ECM components, eventually resulting in the premature aging of the skin [19]. Growing evidence suggests the strategies for the prevention of skin photoaging are blocking UV from penetrating the skin layer, inhibiting ROS generation and inflammatory mediators, and inhibiting the gene activations of the MMPs [20]. Cutaneous moisture is another crucial factor in skin health and is connected to the stratum corneum, which functions as a barrier to skin water. Healthy skin retains more than 10% skin moisture. However, sunlight and UV irradiation cause skin moisture to decline below normal levels, thereby leading to dried and rough-textured skin, desquamation, and itching [21]. Given the consistency of the detrimental effects of UVB on the skin, the current study revealed that UVB induced severe wrinkle formation in the dorsal back skin of SKH1-hr hairless mice. Moreover, there was a significant increase in both wrinkle length and depth of wrinkles, as well as loss of the skin water contents compared to the unexposed UVB intact control. Histopathological analysis also showed a thickened epidermal layer and an increased formation of microfolds due to UVB irradiation. These manifestations of photoaging due to UVB, such as wrinkle formation, epidermal thickening, and loss of skin water, were mitigated by UAE. The alterations that occur during photoaging are known to be caused by an imbalance between the synthesis and degradation of components, such as collagen, elastin, and glycosaminoglycan, constituting the ECM in the dermal layer of the skin [22]. Indeed, wrinkle formation during the photoaging process is closely linked to the degradation of ECM components due to the activation of MMPs [20,23]. Fibrillary collagen is cleaved by MMP1 or MMP13 and further degraded by MMP9, which leads to the accumulation of decomposed collagen fragments in skin tissue. Recent evidence indicates that the direct inhibition or gene regulation of MMPs can be a promising therapeutic target for photoaging and photocarcinogenesis [20,24]. The present results showed that UAE inhibited the accumulation of decomposed collagen fibers in MT staining and recovered skin COL1 contents, the most abundant fibrous protein in the ECM, against UVB irradiation by inducing *COL1A1* and *COL1A2* mRNA expressions. Moreover, UAE inhibited the UVB-induced mRNA expressions of *MMP1*, *MMP9*, and *MMP13*. These results are in line with a recent study on MMP1 inhibition and type I procollagen-inducing effects of polyphenols in unripe apples on UVB-irradiated human skin fibroblasts [13]. Therefore, the anti-wrinkle formation effect of UAE may be due to the suppression of COL1 degradation through MMP gene regulation.

A dramatic alteration observed during skin aging is the reduction in hyaluronic acid, responsible for binding and retaining water molecules, which causes the depletion of skin water [25]. Oral intake of hyaluronic acid can help to recover water loss in the stratum corneum of the face [26]. Under UVB irradiation, the reduced HAS2 gene expression is downregulated in skin fibroblasts, resulting in a reduction in hyaluronic acid synthesis [27]. The results of this study demonstrated that UAE increased hyaluronic acid contents in skin tissue via the upregulation of the HAS gene family expression. Thus, UAE contributed to improving the UVB-induced loss of skin water by increasing hyaluronic acid through HAS gene regulation.

UVB, the most energetic UV wavelength, directly causes DNA breakdown and induces ROS generation, which leads to DNA damage, lipid peroxidation, and impairment of mitochondrial membrane potential, ultimately inducing apoptosis of epidermal keratinocytes and dermal fibroblast [19]. The death of these skin cells results in the breakdown of ECM components through MMP activation and the secretion of inflammatory cytokines, which accelerates skin aging [19]. In the present study, UAE inhibited apoptosis in the UVB-exposed dorsal back skin tissue of mice, as assessed by immunohistostaining using cleaved caspase-3 and cleaved PARP antibodies. UV radiation generates two primary types of DNA damage, cyclobutene pyrimidine dimers (CPD) and pyrimidine 6-4 pyrimidone photoproducts (6-4PP) [28]. The main cellular response to 6-4PP is the activation of the apoptosis pathway, whereas the response to CPD seems to mainly involve cell cycle arrest [28]. Although UAE inhibited UVB-induced apoptosis in mice tissue, further research is required to determine the details of the UAE and UV-induced DNA photoproducts. Our data also showed UAE alleviated UVB-induced reduction of GSH content by upregulating the gene expression of *GSH reductase* and inhibited UVB-induced lipid peroxidation and superoxide anion production through the transcriptional regulation of *NOX2*. Immunohistochemical analysis using NT or 4-HNE staining demonstrated potent antioxidant activities of UAE. The degradation of ECM during photoaging is closely related to ROS-mediated cellular responses [29]. Specifically, the expression of MMP1 is increased by UV irradiation, which is also stimulated by ROS, and plays a decisive role in photoaging [20,24]. The antioxidant activity of UAE may contribute to the effects of UAE on ECM protein regulation. In addition, p53/p21 pathway can contribute to cellular adaptive responses to UVB damage associated with DNA repair, cell cycle arrest, and apoptosis [30]. UVB exposure can suppress p21 expression associated with increased apoptosis, whereas p21 overexpression may serve to reduce antioxidant defense capacity against UVB irradiation [31]. In the current study, UAE showed significant inhibitory effects on lipid peroxidation and apoptosis in UVB-irradiated dorsal back tissue of mice, but the detailed underlying molecular mechanisms related to the p53/p21 pathway require further study.

UAE alleviated UVB-induced skin edema as the local inflammatory state of the skin and inhibited the UVB-induced neutrophil inflammatory response (MPO activity) in the skin. The infiltration of inflammatory cells, including neutrophils, may contribute to regulate MMP expression [20]. UV radiation triggers the secretion of IL-1 to initiate the inflammatory response in the skin and inhibits IL-10 to promote the survival of skin cells damaged by UV irradiation [20,32]. Our data showed that UAE reduced the UVB-induced IL-1β secretion, whereas it increased the release of IL-10. UV can trigger ROS-mediated inflammatory responses through the activation of several kinase cascades, such as Akt, JNK, ERK, and p38 mitogen-activated protein kinase (MAPK). UVB irradiation activates Akt, and p38 MAPK, and triggers underlying inflammatory responses, as well as UVB-induced apoptosis of keratinocytes, which is primarily associated with p38 MAPK activation rather than JNK or ERK [33]. Therefore, the regulation of Akt and p38 MAPK may contribute to preventing UVB-induced skin cell damage, including oxidative stress, inflammation, and apoptosis [34,35]. Activator protein 1 (AP-1), activated by MAPK, leads to inflammatory processes and the degradation of collagen through MMP activation in the skin [29]. The transcriptional regulatory regions in the MMP genes include an AP-1 regulatory element. AP-1 suppresses the transforming growth factor-β (TGF-β)-Smad signaling pathway, thereby reducing collagen synthesis [24]. According to the results of this study, UAE also downregulated *AKT* and *p38 MAPK* gene expression, while upregulating *TGF-β* gene expression (Figure S2). This finding might indicate the mechanism responsible for the protective effects of UAE against UVB-induced inflammation, collagen degradation, and apoptosis in the skin. UV activates p38 MAPK dependent cyclooxygenase-2 (COX-2) induction, which serves to regulate prostaglandin E2 secretion, responsible for immune cell infiltration, and edema [19]. Phloridzin has been reported to attenuate UVB-induced ROS generation and cyclooxygenase-2 expression and consequent excessive inflammation response through the regulation of JNK and p38 MAPK [36]. In this study,

UAE inhibited UVB-induced skin edema and neutrophil inflammatory response in the skin, and downregulated p38 MAPK gene expression.

Polyphenols exert potent antioxidant activity and inhibitory effects on the degradation of ECM components. Consequently, oral intake of polyphenol may help alleviate skin photoaging [11]. As apples ripen, their antioxidant activities and the polyphenol content decrease, and the chlorogenic acid content is suggested to affect the antioxidant activities of apples [17]. Another study suggests that unripe apple extract contained 63.8% procyanidin in its polyphenol profile, and that antioxidant activity of unripe apple extract against UV irradiation was mainly due to procyanidin [8]. The present study identified that UAE contained phloridzin (0.06 mg/g) (Figure S1), which may contribute to the antioxidant and anti-inflammation effects of UAE on UVB-induced skin aging. However, depending on the manufacturing process of an extract, the content of the polyphenols may differ. Thus, further research should be undertaken to identify the exact composition and content of polyphenols in UAE.

5. Conclusions

In this study, we tried to investigate the effects of UAE in preventing UVB-irradiated skin photoaging. We demonstrated that oral administration of UAE mitigated UVB-induced wrinkle formation, loss of skin water, collagen degradation, and skin edema through its the anti-inflammatory, anti-apoptotic, and antioxidant properties, which were comparable to those of L-AA (100 mg/kg) at the same oral dose level. These findings suggest that UAE may be a therapeutic candidate or natural resource for functional products to prevent skin photoaging.

Supplementary Materials: The following supporting information can be downloaded at: https://www.mdpi.com/article/10.3390/app13084788/s1, Table S1: UAE preparation procedure; Table S2: Oligonucleotide sequences used in the present study; Figure S1: Identification of UAE by high-performance liquid chromatography (HPLC); Figure S2: *TGF-b1*, *p38 MAPK*, and *AKT* mRNA expression levels in dorsal back skin tissues were quantified by real-time PCR.

Author Contributions: H.R.P. and J.K.K. contributed to the study plan, data collection, analysis, manuscript writing. J.K.L. and B.R.C. contributed to the biological data analysis, result discussion and proofreading. S.K.K. contributed to the histopathological assessment. K.H.J. contributed to the study plan, result discussion, manuscript reviewing and editing, and supervision. All authors have read and agreed to the published version of the manuscript.

Funding: This research received no external funding.

Institutional Review Board Statement: The animal study protocol was approved by the Institutional Animal Care and Use Committee of the Daegu Haany University (Approval No. DHU2021-030).

Informed Consent Statement: Not applicable.

Data Availability Statement: Not applicable.

Conflicts of Interest: The authors declare no conflict of interest.

References

1. Zhang, S.; Duan, E. Fighting against Skin Aging: The Way from Bench to Bedside. *Cell Transpl.* **2018**, *27*, 729–738. [CrossRef] [PubMed]
2. Uitto, J. Understanding premature skin aging. *N. Engl. J. Med.* **1997**, *337*, 1463–1465. [CrossRef] [PubMed]
3. Salminen, A.; Kaarniranta, K.; Kauppinen, A. Photoaging: UV radiation-induced inflammation and immunosuppression accelerate the aging process in the skin. *Inflamm. Res.* **2022**, *71*, 817–831. [CrossRef]
4. Pedić, L.; Pondeljak, N.; Šitum, M. Recent information on photoaging mechanisms and the preventive role of topical sunscreen products. *Acta Dermatovenerol. Alp. Pannonica Adriat.* **2020**, *29*, 201–207. [CrossRef]
5. Ahmed, I.A.; Mikail, M.A.; Zamakshshari, N.H.; Mustafa, M.R.; Hashim, N.M.; Othman, R. Trends and challenges in phytotherapy and phytocosmetics for skin aging. *Saudi J. Biol. Sci.* **2022**, *29*, 103363. [CrossRef]
6. Michalak, M.; Pierzak, M.; Krecisz, B.; Suliga, E. Bioactive Compounds for Skin Health: A Review. *Nutrients* **2021**, *13*, 203. [CrossRef] [PubMed]

7. Kojima, T.; Akiyama, H.; Sasai, M.; Taniuchi, S.; Goda, Y.; Toyoda, M.; Kobayashi, Y. Anti-allergic effect of apple polyphenol on patients with atopic dermatitis: A pilot study. *Allergol. Int.* **2000**, *49*, 69–73. [CrossRef]
8. Shoji, T.; Masumoto, S.; Moriichi, N.; Ohtake, Y.; Kanda, T. Administration of Apple Polyphenol Supplements for Skin Conditions in Healthy Women: A Randomized, Double-Blind, Placebo-Controlled Clinical Trial. *Nutrients* **2020**, *12*, 1071. [CrossRef]
9. Koutsos, A.; Riccadonna, S.; Ulaszewska, M.M.; Franceschi, P.; Trošt, K.; Galvin, A.; Braune, T.; Fava, F.; Perenzoni, D.; Mattivi, F.; et al. Two apples a day lower serum cholesterol and improve cardiometabolic biomarkers in mildly hypercholesterolemic adults: A randomized, controlled, crossover trial. *Am. J. Clin. Nutr.* **2020**, *111*, 307–318. [CrossRef]
10. Bondonno, N.P.; Bondonno, C.P.; Blekkenhorst, L.C.; Considine, M.J.; Maghzal, G.; Stocker, R.; Woodman, R.J.; Ward, N.C.; Hodgson, J.M.; Croft, K.D. Flavonoid-Rich Apple Improves Endothelial Function in Individuals at Risk for Cardiovascular Disease: A Randomized Controlled Clinical Trial. *Mol. Nutr. Food Res.* **2018**, *62*, 1700674. [CrossRef]
11. Menaa, F.; Menaa, A.; Tréton, J. Chapter 63—Polyphenols against Skin Aging. In *Polyphenols in Human Health and Disease*; Watson, R.R., Preedy, V.R., Zibadi, S., Eds.; Academic Press: San Diego, CA, USA, 2014; pp. 819–830.
12. Piccinino, D.; Capecchi, E.; Delfino, I.; Crucianelli, M.; Conte, N.; Avitabile, D.; Saladino, R. Green and Scalable Preparation of Colloidal Suspension of Lignin Nanoparticles and Its Application in Eco-friendly Sunscreen Formulations. *ACS Omega* **2021**, *6*, 21444–21456. [CrossRef]
13. Park, E.K.; Ahn, S.R.; Kim, D.-H.; Lee, E.-W.; Kwon, H.J.; Kim, B.W.; Kim, T.H. Effects of unripe apple polyphenols on the expression of matrix metalloproteinase-1 and type-1 procollagen in ultraviolet irradiated human skin fibroblasts. *J. Korean Soc. Appl. Biol. Chem.* **2014**, *57*, 449–455. [CrossRef]
14. Bradley, P.P.; Priebat, D.A.; Christensen, R.D.; Rothstein, G. Measurement of cutaneous inflammation: Estimation of neutrophil content with an enzyme marker. *J. Investig. Derm.* **1982**, *78*, 206–209. [CrossRef] [PubMed]
15. Jegal, K.H.; Kim, E.O.; Kim, J.K.; Park, S.M.; Jung, D.H.; Lee, G.H.; Ki, S.H.; Byun, S.H.; Ku, S.K.; Cho, I.J.; et al. Luteolin prevents liver from tunicamycin-induced endoplasmic reticulum stress via nuclear factor erythroid 2-related factor 2-dependent sestrin 2 induction. *Toxicol. Appl. Pharm.* **2020**, *399*, 115036. [CrossRef]
16. Kim, Y.I.; Oh, W.S.; Song, P.H.; Yun, S.; Kwon, Y.S.; Lee, Y.J.; Ku, S.K.; Song, C.H.; Oh, T.H. Anti-Photoaging Effects of Low Molecular-Weight Fucoidan on Ultraviolet B-Irradiated Mice. *Mar. Drugs* **2018**, *16*, 286. [CrossRef]
17. Zheng, H.-Z.; Kim, Y.-I.; Chung, S.-K. A profile of physicochemical and antioxidant changes during fruit growth for the utilisation of unripe apples. *Food Chem.* **2012**, *131*, 106–110. [CrossRef]
18. Choi, J.-H.; Chung, S.-K. Antioxidant and antimicrobial activities of polyphenols isolated from unripe apples (*Malus pumila* cv. Hongro). *Korean J. Food Preserv.* **2019**, *26*, 690–696. [CrossRef]
19. Ansary, T.M.; Hossain, M.R.; Kamiya, K.; Komine, M.; Ohtsuki, M. Inflammatory Molecules Associated with Ultraviolet Radiation-Mediated Skin Aging. *Int. J. Mol. Sci.* **2021**, *22*, 3974. [CrossRef]
20. Pillai, S.; Oresajo, C.; Hayward, J. Ultraviolet radiation and skin aging: Roles of reactive oxygen species, inflammation and protease activation, and strategies for prevention of inflammation-induced matrix degradation—A review. *Int. J. Cosmet. Sci.* **2005**, *27*, 17–34. [CrossRef]
21. Verdier-Sevrain, S.; Bonte, F. Skin hydration: A review on its molecular mechanisms. *J Cosmet. Derm.* **2007**, *6*, 75–82. [CrossRef]
22. Uitto, J.; Bernstein, E.F. Molecular Mechanisms of Cutaneous Aging: Connective Tissue Alterations in the Dermis. *J. Investig. Dermatol. Symp. Proc.* **1998**, *3*, 41–44. [CrossRef]
23. Naylor, E.C.; Watson, R.E.; Sherratt, M.J. Molecular aspects of skin ageing. *Maturitas* **2011**, *69*, 249–256. [CrossRef]
24. Pittayapruek, P.; Meephansan, J.; Prapapan, O.; Komine, M.; Ohtsuki, M. Role of Matrix Metalloproteinases in Photoaging and Photocarcinogenesis. *Int. J. Mol. Sci.* **2016**, *17*, 868. [CrossRef]
25. Papakonstantinou, E.; Roth, M.; Karakiulakis, G. Hyaluronic acid: A key molecule in skin aging. *Dermatoendocrinology* **2012**, *4*, 253–258. [CrossRef]
26. Sun, Q.; Wu, J.; Qian, G.; Cheng, H. Effectiveness of Dietary Supplement for Skin Moisturizing in Healthy Adults: A Systematic Review and Meta-Analysis of Randomized Controlled Trials. *Front. Nutr.* **2022**, *9*, 895192. [CrossRef] [PubMed]
27. Wang, Y.; Lauer, M.E.; Anand, S.; Mack, J.A.; Maytin, E.V. Hyaluronan synthase 2 protects skin fibroblasts against apoptosis induced by environmental stress. *J. Biol. Chem.* **2014**, *289*, 32253–32265. [CrossRef] [PubMed]
28. Lo, H.L.; Nakajima, S.; Ma, L.; Walter, B.; Yasui, A.; Ethell, D.W.; Owen, L.B. Differential biologic effects of CPD and 6-4PP UV-induced DNA damage on the induction of apoptosis and cell-cycle arrest. *BMC Cancer* **2005**, *5*, 135. [CrossRef]
29. Wolfle, U.; Seelinger, G.; Bauer, G.; Meinke, M.C.; Lademann, J.; Schempp, C.M. Reactive molecule species and antioxidative mechanisms in normal skin and skin aging. *Ski. Pharm. Physiol.* **2014**, *27*, 316–332. [CrossRef]
30. Verschooten, L.; Declercq, L.; Garmyn, M. Adaptive response of the skin to UVB damage: Role of the p53 protein. *Int. J. Cosmet. Sci.* **2006**, *28*, 1–7. [CrossRef] [PubMed]
31. Chen, A.; Huang, X.; Xue, Z.; Cao, D.; Huang, K.; Chen, J.; Pan, Y.; Gao, Y. The Role of p21 in Apoptosis, Proliferation, Cell Cycle Arrest, and Antioxidant Activity in UVB-Irradiated Human HaCaT Keratinocytes. *Med. Sci. Monit. Basic Res.* **2015**, *21*, 86–95. [CrossRef] [PubMed]
32. Weiss, E.; Mamelak, A.J.; La Morgia, S.; Wang, B.; Feliciani, C.; Tulli, A.; Sauder, D.N. The role of interleukin 10 in the pathogenesis and potential treatment of skin diseases. *J. Am. Acad. Derm.* **2004**, *50*, 657–675; quiz 676–678. [CrossRef] [PubMed]

33. Nakamura, S.; Takahashi, H.; Kinouchi, M.; Manabe, A.; Ishida-Yamamoto, A.; Hashimoto, Y.; Iizuka, H. Differential phosphorylation of mitogen-activated protein kinase families by epidermal growth factor and ultraviolet B irradiation in SV40-transformed human keratinocytes. *J. Derm. Sci.* **2001**, *25*, 139–149. [CrossRef] [PubMed]
34. Kim, A.L.; Labasi, J.M.; Zhu, Y.; Tang, X.; McClure, K.; Gabel, C.A.; Athar, M.; Bickers, D.R. Role of p38 MAPK in UVB-induced inflammatory responses in the skin of SKH-1 hairless mice. *J. Investig. Derm.* **2005**, *124*, 1318–1325. [CrossRef]
35. Kunchana, K.; Jarisarapurin, W.; Chularojmontri, L.; Wattanapitayakul, S.K. Potential Use of Amla (*Phyllanthus emblica* L.) Fruit Extract to Protect Skin Keratinocytes from Inflammation and Apoptosis after UVB Irradiation. *Antioxidants* **2021**, *10*, 703. [CrossRef] [PubMed]
36. Zhai, Y.; Dang, Y.; Gao, W.; Zhang, Y.; Xu, P.; Gu, J.; Ye, X. P38 and JNK signal pathways are involved in the regulation of phlorizin against UVB-induced skin damage. *Exp. Derm.* **2015**, *24*, 275–279. [CrossRef]